



Synthesis of nanostructured NiO and its application in laser-induced photocatalytic reduction of Cr(VI) from water

M. Qamar^a, M.A. Gondal^{a,b,*}, Z.H. Yamani^{a,b}

^a Center of Excellence in Nanotechnology, King Fahd University of Petroleum and Minerals, KFUPM Box 741, Dhahran 31261, Saudi Arabia

^b Laser Research Group, Physics Department, King Fahd University of Petroleum and Minerals, Dhahran 31261, Saudi Arabia

ARTICLE INFO

Article history:

Received 21 July 2010

Received in revised form 28 March 2011

Accepted 30 March 2011

Available online 9 April 2011

Keywords:

Photocatalysis

Chromium reduction

Nanostructured NiO

Water purification

Laser applications

ABSTRACT

Owing to its high toxicity, chromium(VI) is considered as top priority pollutant for many countries in the world and removal of this pollutant from waste water is highly desirable. The present investigation addresses the synthesis of NiO nanoparticles using sol–gel method and their application in heterogeneous photocatalytic reduction of Cr(VI) using a 355 nm laser radiation generated from Nd:YAG laser. The study showed that ~90% Cr(VI) was removed within short laser exposure time (75 min) in presence of nanostructured NiO without the use of any additive as reported in other studies. Effect of critical parameters, such as calcination temperature, calcination time, laser energy, catalyst amount, chromium concentration, and added electron donor and acceptor on the photocatalytic reduction process was investigated. The photocatalytic reduction of metal was found to be strongly dependant on the above mentioned parameters.

© 2011 Elsevier B.V. All rights reserved.

1. Introduction

Chromium has been used extensively in several industries, such as alloys and steel manufacturing, metal plating, military purposes, and tanning of leather, as well as in the pigment and refractory industries [1,2]. The increasing level of chromium(VI) metal ion in the environment is a great concern to the societies and regulation authorities around the world. The toxicity and carcinogenic properties of chromium(VI) have been known for a long time [3] and it is in the list of priority pollutants of many countries in the world [4]. Conventionally, industrial waste treatments for heavy metal removal include techniques such as biological treatment, ion exchange, liquid–liquid extraction, precipitation, reverse osmosis, and activated carbon adsorption [5]. However, these techniques often utilize potentially hazardous or polluting materials and can only transform the pollutants from one phase to another [6]. Moreover, they may require pretreatment, their by-products are often considered hazardous, and their disposal is costly.

Heterogeneous photocatalysis involving semiconductors has attracted considerable attention in recent years for the remediation of undesirable pollutants both in aqueous [7–11] and gaseous phase [12–14] using solar or artificial light sources. The photocat-

alytic processes using semiconductors have demonstrated the need to overcome the limitations in achieving higher photonic efficiencies. The fundamentals of heterogeneous photocatalytic oxidation processes have been discussed extensively in the literature [15,16]. Briefly, when a photocatalyst absorbs a photon of energy equal to or greater than its band gap, an electron is promoted from the valence band to the conduction band (e^-cb) leaving behind an electron vacancy or “hole” in the valence band (h^+vb). If the charge separation is maintained, the electron and hole may migrate to the catalyst surface where they participate in redox reactions with adsorbed species. It has been reported that the photocatalytic reduction of highly toxic Cr(VI) into non-toxic Cr(III) can be achieved with the help of semiconductors and light under certain conditions [17–21].

Although the efforts have been made to investigate the reduction of metal using semiconductor-mediated photocatalytic process, most of the studies have been carried out using some organic additives such as salicylic acid, oxalate, phenols, dye, and humic acid [22–25], as well as some electron donor such as methanol, formate ions, etc. [5,26]. It is worth mentioning that all the previous work on reduction of heavy metals from waste water using heterogeneous photocatalysis has been carried out with broad spectral radiation sources such as lamps and TiO₂ as a photocatalyst where the reduction and/or precipitation of metal ions was found to be negligible in the absence of organic additives. Moreover, certain problems are associated with the use of lamps emitting over broad spectral wavelength range such as the long term power stability due to over heating of lamps during the operation, low photonic efficiency, etc. for complete mineralization of

* Corresponding author at: Laser Research Group, Physics Department, King Fahd University of Petroleum and Minerals, Dhahran 31261, Saudi Arabia.
Tel.: +966 38602351; fax: +966 38602293.

E-mail address: magondal@kfupm.edu.sa (M.A. Gondal).

pollutants. Keeping in view the long term stability of lamps, it is of interest to use laser radiations as an excitation source to study the activity of photocatalysts because laser light has unique properties like mono-chromaticity, high intensity, and low beam divergence. However, the initial cost of laser based systems will be much higher than lamp based systems. The main purpose of using laser in this work is to study the performance of the NiO catalyst in short span of time and other experimental parameters as compared to lamps for effective reduction of Cr(VI) from water. However for commercial scale applications of water purification, lasers are not suitable and one can use the solar radiations. Furthermore, we are not claiming in this work that lasers are the best alternatives for other irradiation sources.

To the best of our knowledge, complete and efficient photocatalytic reduction of Cr(VI) in the presence of nanostructured NiO without the use of any additive has not been reported so far. The present study describes the synthesis of NiO nanoparticles following sol–gel method and their application in reduction of Cr(VI) from water system using a 355 nm laser irradiation. The dependence of the metal reduction from water on calcination temperature, calcination time, laser irradiation energy, catalyst amount, chromium concentration, electron donor and acceptor was investigated. The data concerning temporal behavior of metal reduction was fitted to first-order kinetic and reaction rate was estimated.

2. Experimental

2.1. Chemicals

Potassium dichromate ($K_2Cr_2O_7$) was obtained from Sigma–Aldrich. Nickel acetate was obtained from Fluka and oxalic acid was purchased from Fisher Scientific Company. The other chemicals H_2O_2 and alcohols (ethanol and methanol) were obtained from Merck.

2.2. Synthesis of NiO nanoparticles

The synthesis of NiO nanoparticles was carried out adopting sol–gel method. For this purpose, nickel acetate tetrahydrate ($(CH_3COO)_2Ni \cdot 4H_2O$) was dissolved in ethanol under constant stirring for 2 h at 40–45 °C to obtain a clear and light greenish sol. Oxalic acid solution (0.23 M in ethanol) is then added slowly to the warm sol to yield a greenish thick gel. The thick gel was then refluxed at 80–90 °C for 24 h under vigorous stirring in the air atmosphere. It was further dried in an oven by heating at 110 °C for whole night. Dried gel/product was grinded into fine powders and calcined in a tube furnace from 300 °C to 700 °C for different time periods to obtain nanocrystalline NiO. This process produced a fine black powder.

2.3. Characterization

Characterization of the synthesized nanostructure NiO was carried out employing Field Emission Electron Microscope, Transmission Electron Microscope (JEOL, JEM-2100F), X-ray Diffractometer (Shimadzu 6000 using Cu–K radiation, with operating voltage of 40 kV and current of 30 mA), Particle Size Analyzer (Microtrac, S3500). The absorbance of the samples was monitored by measuring the absorbance on a UV–Vis spectrophotometer (JASCO).

2.4. Evaluation of photocatalytic activity

Stock solutions of the potassium dichromate containing desired concentrations were prepared in distilled water. For irradiation experiments, 100 mL solution of desired concentration of the model pollutant was taken into the reaction vessel and the required

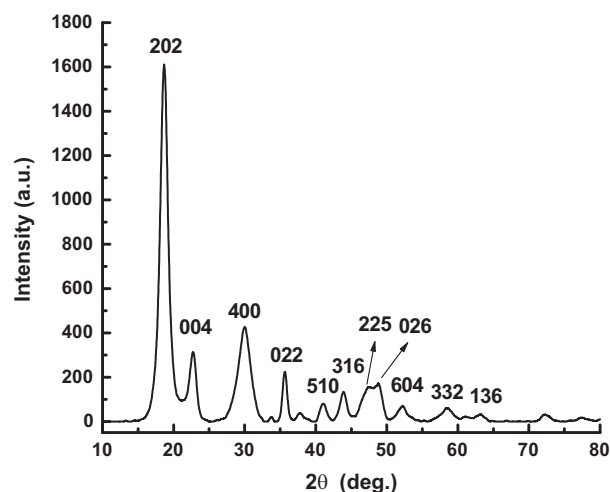


Fig. 1. XRD patterns of nickel acetate dihydrate ($NiC_2O_4 \cdot 2H_2O$) obtained after drying the gel-product at 110 °C for 12 h.

amount of photocatalyst was added and the solution was stirred for at least 15 min in the dark. The pH of the reaction mixture was adjusted to ~ 7 by adding a dilute aqueous solution of HNO_3 or NaOH. The zero time reading was obtained from a blank solution kept in the dark but otherwise treated similar to the irradiated solution. Irradiations were carried out using a 355 nm wavelength high power laser beam generated from the third harmonic of the Spectra Physics Nd:YAG laser (Model GCR 250), with a pulse width of ~ 8 ns. In order to avoid the destructive effect of radiation, laser beam diameter was expanded to 1.0 cm. A schematic of the experimental set-up was documented in our earlier publications [27,28]. Samples (3 mL) were collected before and at regular time intervals during the irradiation. The catalyst was removed through filtration before the analysis.

2.5. Analysis

The reduction of Cr(VI) was monitored by measuring the absorbance on a UV–Vis spectrophotometer. The absorption maxima of the potassium dichromate was found to be 372 nm. The reduction of the metal, therefore, was estimated at this wavelength as a function of irradiation time. For each experiment, the rate for the reduction of the model pollutant was calculated from the initial slope obtained by linear regression from a plot of the natural logarithm of absorbance of the metal as a function of irradiation time, i.e. first order reduction kinetics.

3. Results and discussion

3.1. Structural and morphological characterization of NiO nanoparticles

The XRD pattern of the dried gel obtained after drying at 110 °C for 12 h has been depicted in Fig. 1. The XRD patterns corresponded to the formation of nickel oxalate dihydrate ($NiC_2O_4 \cdot 2H_2O$) having an orthorhombic structure with lattice parameters $a = 11.84 \text{ \AA}$, $b = 5.345 \text{ \AA}$, $c = 15.716 \text{ \AA}$, $Z = 8$, and space group Cccm [29]. This result contradicts the result obtained by Wang et al. [30] where the formation of nickel oxalate hydrate was observed following the similar sol–gel method with only difference that nickel nitrate instead of nickel acetate was used as precursor. Fig. 2 illustrates the FESEM and TEM micrographs of nanostructured nickel oxide calcined at 400 °C for 2 h. The microscopic study indicated that all the particles

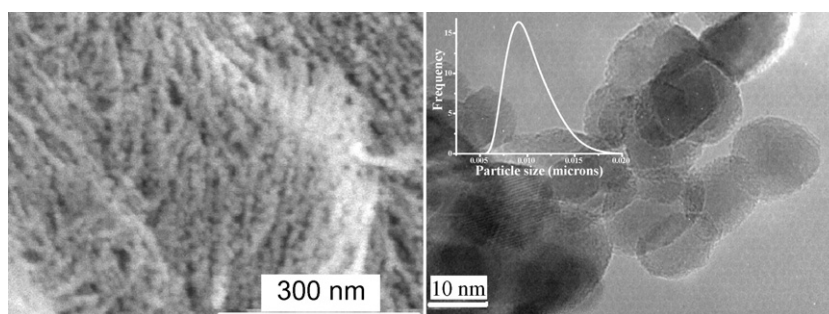


Fig. 2. FESEM and TEM images of nanostructured NiO calcined at 400 °C for 2 h. Figure inset: particle size distribution.

Table 1

Effect of calcination temperature, heating time on the photocatalytic reduction of Cr(VI) in the presence of NiO nanoparticles.

Calcination temperature (°C)	Heating time (h)	Average particle size (nm)	Rate constant (min ⁻¹)	Experimental conditions
300	2	07.0	0.009	Laser energy = 240 mJ, chromium concentration = 50 mg/L, NiO concentration = 1.0 g/L, irradiation time = 75 min.
400	2	09.5	0.026	
500	2	20.0	0.021	
600	2	55.0	0.016	
700	2	125.0	0.010	
400	1	07.5	0.015	
400	3	12.5	0.023	
400	4	17.0	0.018	
400	5	24.0	0.014	

were spherical in shape and were in the range 8–15 nm. The average particle size of the calcined NiO samples at different temperatures and times were determined using particle size analyzer and the obtained values are listed in Table 1. A representative example of particle size analysis of the NiO sample calcined at 400 °C for 2 h is presented as inset figure in Fig. 2. It can be seen that the average particle size determined by the particle size analyzer is almost similar to that obtained by TEM. The structural evolution of nickel oxalate dihydrate as a function of calcination temperatures from 300 to 700 °C for 2 h was recorded through XRD and obtained results are illustrated in Fig. 3. The patterns corresponded to the formation NiO with fcc structure and improvement in its crystallinity with increasing temperature.

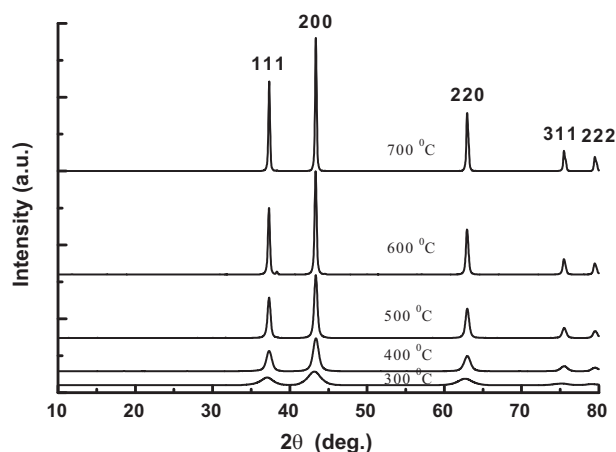


Fig. 3. XRD patterns of the NiO samples obtained after calcination at different temperatures for 2 h.

3.2. Photolysis of NiO suspensions containing potassium dichromate

Fig. 4a shows the typical UV absorption spectrum illustrating the trend of reduction of Cr(VI) in presence of NiO with as a function of time under laser irradiation. It can be seen from the figure that about 90% Cr(VI) was removed within short laser exposure time (75 min) using 355 nm laser radiations. In order to determine the role of photocatalyst in the reduction process, blank experiment was also carried out by irradiating the aqueous solution of the potassium dichromate under laser light in the absence of NiO where about 5% reduction was observed.

For each experiment, the rate constant was calculated from the plot of natural logarithm of pollutant concentration as a function of irradiation time. A typical plot of $-\ln A/A^0$ (for Fig. 4a) versus time is depicted in Fig. 4b for Cr(VI) reduction. The least square fit $R = 0.97$.

3.3. Effect of calcination temperature and time on the photocatalytic reduction process

The photocatalytic activity of NiO samples obtained after heating at different calcination temperatures from 300 to 700 °C as well as different heating times was also evaluated and obtained values are listed in Table 1. It can be noticed from Table 1 that the photocatalytic activity of samples increases with increasing calcination temperature presumably due to the improvement of crystallinity, and the samples calcined at 400 °C showed the best activity for the reduction of Cr(VI) followed by a decrease at higher temperatures. The best activity shown by the sample calcined at 400 °C may be mainly attributed to the generation and separation of charge carriers (e^- and h^+) which is affected by various properties, such as crystallinity, surface area, and particle size, of the materials (given the fact that with increasing calcination temperature and time, the particle size increases and surface area decreases) [7,31]. Briefly, in the photocatalytic process, the separated charge

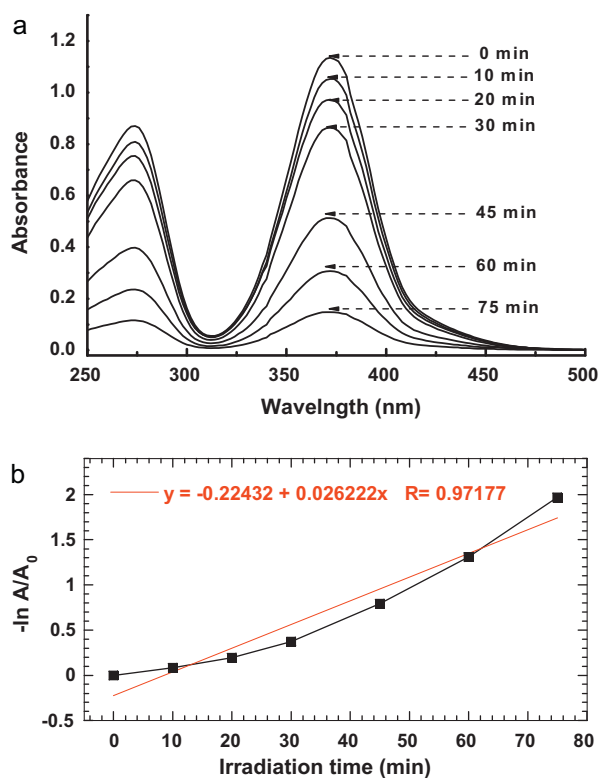


Fig. 4. (a) Typical UV-vis spectra showing the change in absorption intensity as a function of laser irradiation time for an aqueous solution of $K_2Cr_2O_7$ in the presence of NiO. (b) A plot of $-\ln A/A_0$ versus the reaction time (for (a)) for Cr(VI) reduction showing the first-order kinetics.

carriers escape to the particle surface (surface-trapped charge carriers) where they participate in redox reactions with the adsorbed species (interfacial-charge transfer process). When the particle size of the sample is very small, surface-trapped charge carriers may get annihilated by the subsequent photo-generated e^-/h^+ pair before the interfacial-charge transfer process takes place which in turn leads the lower performance of the catalyst. When, on the other hand, the crystallite size is larger, the photo-induced e^-/h^+ have to travel much distance to reach the surface and this extended journey increases the possibility of recombination within the particle volume. When the size of the particles are neither very small nor too large, the generated e^-/h^+ pair may move to the surface of particles and get trapped before they undergo volume charge-carrier recombination process (surface charge carrier trapping). For the optimum photocatalytic performance, therefore, the rate of volume and surface charge carrier recombination process should be minimum, while that of the interfacial-charge transfer process should be maximum. Similar explanation can also be offered for the best activity shown by the NiO sample heated at $400^\circ C$ for 2 h as compared to those heated for 1, 3, 4, and 5 h.

3.4. Effect of incident laser energy on the photocatalytic reduction process

The effect of incident laser energy on the reduction of Cr(VI) was investigated and obtained results are presented in Table 2. It is obvious from Table 2 that the reduction of metal was significantly influenced by the laser energy and reduction was found to increase almost linearly with the increase in laser energy within the range studied. This phenomenon may be explained in terms of the fact that when higher laser energy is employed, incident photon flux increases in the solution exciting more and more catalyst particles

Table 2

Laser-induced photocatalytic reduction of Cr(VI) in aqueous suspensions of NiO under different experimental conditions.

Parameter	Rate constant (min^{-1})	Experimental conditions
Laser energy (mJ)		
70.00	0.0002	Chromium concentration = 50 mg/L, NiO concentration = 1.0 g/L, irradiation time = 75 min.
110.0	0.0005	
150.0	0.0013	
200.0	0.0019	
240.0	0.0026	
Cr(VI) concentration		
25.00	0.0017	Laser energy = 240 mJ, NiO concentration = 1.0 g/L, irradiation time = 75 min.
50.00	0.0026	
75.00	0.0021	
100.0	0.0011	
Catalysts amount (g L^{-1})		
0.5	0.0009	Laser energy = 240 mJ, chromium concentration = 50 mg/L, irradiation time = 75 min.
1.0	0.0026	
2.0	0.0039	
3.0	0.0045	
4.0	0.0048	
5.0	0.0043	

which in turn increases the photocatalytic reduction process. It is pertinent to mention here that the maximum energy we can get with the laser we have is about 240 mJ and hence the effect of laser energy more than 240 mJ could not be investigated in the present study. In contrast to the conventional photocatalytic systems where one has to change the lamp to control the energy, the laser equipment furnishes very easy access as well as a range of energy to control the photonic efficiencies, according to the requirements, during the photocatalytic reactions. It has been observed in this study that the reduction of chromium metal can be significantly enhanced (almost complete reduction within the 75 min of irradiation time) by simply increasing the laser energy. The observed improvement in the reduction trend of Cr(VI) as a function of laser energy is more significant than that obtained using different conventional UV lamps [32].

3.5. Effect of Cr(VI) concentration on the photocatalytic reduction process

It is important both from mechanistic and application points of view to study the dependence of the photocatalytic reaction rate on the substrate (pollutant) concentrations. Hence, the influence of substrate concentration varying from 25 mg/L to 130 mg/L on the photocatalytic reduction process was studied and the obtained results are presented in Table 2. It can be seen from Table 2 that the reduction increased with the increase in substrate concentration from 25 to 50 mg/L and a further increase in the concentration of the metal led to a decrease in the reaction rate. The decrease in reduction process at higher metal concentration may be rationalized in terms of the fact that after the reduction of certain amount of metal on the surface of catalyst, the catalyst's surface might get saturated and a further increase in chromium concentration remain in the aqueous solution. Another possible explanation for this behavior may be ascribed to the fact that as the pollutant concentration increases, the color of the irradiating mixture becomes more and more intense (given the fact that the aqueous solution of potassium dichromate produces greenish color) which prevents the penetra-

tion of light to the surface of the catalyst. Hence, the generation of relative amount of reactive species on the surface of the catalyst does not increase as the other parameters such as intensity of light, illumination time and concentration of the catalyst are kept constant. Consequently, the reduction of metal decreases as the concentration exceeds the optimum limit.

3.6. Effect of NiO amount on the photocatalytic reduction process

The dependence of the reduction of metal on the NiO amount is included in Table 2. NiO amount was optimized by exposing the aqueous suspensions of potassium dichromate containing NiO ranging from 50 mg to 500 mg by keeping other parameters constant. As the amount of NiO was increased from 50 to 300 mg, the reaction rate was much faster and a further increase in catalyst loading (from 300 to 400 mg) was not found to be much beneficial for the photocatalytic reduction of metal. When the catalyst amount was increased above 400 mg, the reduction rate of the metal was decreased. As the other parameters, such as exposure to a constant photon flux, beam diameter, stirring rate, metal concentration, irradiation time, etc. were kept constant, further increase in particle density beyond optimum density fails to contribute significantly to the reduction process. When the catalyst amount is very high, after traversing a certain optical path, turbidity impedes further penetration of laser light in the reactor (incidence of the combined phenomena of particle masking and scattering) lowering the efficiency of the catalytic process.

3.7. Effect of added electron donor and acceptor on the photocatalytic reduction process

One practical problem in photocatalytic reactions using semiconductors is the undesired electron/hole recombination, which, in the absence of proper electron acceptor or donor, is extremely efficient and hence represents the major energy-wasting step thus limiting the achievable quantum yield. One strategy to inhibit electron-hole pair recombination is to add other (irreversible) electron acceptors or donor to the reaction. They could have several different effects such as (1) to increase the number of trapped electrons and, consequently, avoid recombination, (2) to generate more radicals and other oxidizing species, and (3) to increase the reduction rate of metals. It is pertinent to mention here that in highly toxic wastewater where the reduction of heavy metal is the major concern, the addition of additives to enhance the photocatalytic process may often be justified. In this connection, we studied the effect of electron acceptor and donor such as hydrogen peroxide and methanol respectively on the photocatalytic reduction of the model pollutant under investigation and the obtained results are shown in Fig. 5. The enhancement in reduction rate of Cr(VI) in the presence of methanol may be ascribed to current-doubling effect [33]. The methanol scavenges the generated holes and get oxidized producing the electron-donating species $\bullet\text{CH}_2\text{OH}$ ($E^0(\bullet\text{CH}_2\text{OH}/\text{CH}_2\text{O}) = -0.95\text{ V}$). Due to its large negative potential, the methanol radical then injects an electron into the semiconductor particles thereby increasing the total number of electrons on the catalyst's surface. The effect of methanol on the metal reduction process, in the absence of photocatalyst, under identical conditions was also investigated. The metal reduction was found to be more or less similar as observed in the case of blank experiment which indicates that the presence of methanol in the absence of catalyst is not effective for the reduction of metal. We also investigated the reduction of metal in presence of NiO and methanol but in the absence of light. The analysis did not indicate any change in chromium concentration. Conversely, the addition of hydrogen peroxide affected the reduction process negatively as evident from Fig. 5. Hydrogen peroxide can pick up the excited electrons mak-

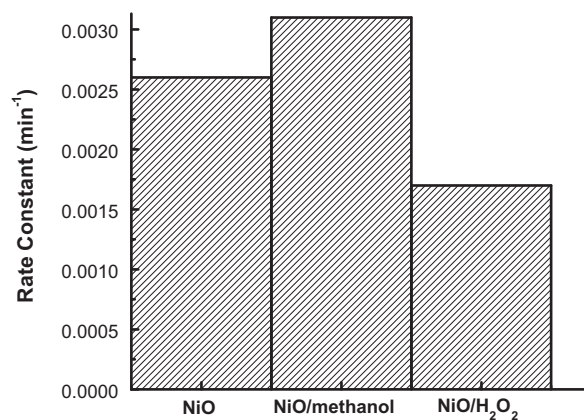


Fig. 5. Effect of electron donor and acceptor on the photocatalytic reduction of Cr(VI).

ing the reduction process slow that was clearly indicated by the retardation of chromium reduction rate.

4. Conclusions

The present investigation showed that the nanostructured NiO synthesized by sol-gel technique can be successfully applied for the complete and efficient reduction of Cr(VI) from aqueous solution using a novel laser-induced photocatalytic process. The study showed that ~90% Cr(VI) was removed within short time (75 min) of laser exposure without the use of any additive. A linear dependence of chromium reduction was found on the incident laser energy. The most appropriate metal concentration for the maximum reduction was found to be about 50 mg/L in this study. The maximum reduction of chromium was achieved using laser energy = 240 mJ and catalyst concentration = 4 g L⁻¹. The addition of electron donor such as methanol enhanced the metal reduction process. This study clearly demonstrated that the NiO-mediated laser-induced photocatalytic process could be applied as an effective method to remove the heavy metals present in waste water in shorter time duration without incorporation of any additives. The optimization of various operational parameters demonstrates the significance of selection of the optimum experimental conditions to obtain a high reduction rate.

Acknowledgements

The support by Center of Excellence in Nanotechnology (CENT) and King Fahd University of Petroleum and Minerals (KFUPM) is gratefully acknowledged under project # 08-NAN-93-4.

References

- [1] L.B. Khailil, W.E. Mourad, M.W. Rophael, *Appl. Catal. B* 17 (1998) 267–273.
- [2] N. Shevchenko, V. Zaitsev, A. Walcarius, *Environ. Sci. Technol.* 42 (2008) 6922–6928.
- [3] D.G. Barceloux, D. Barceloux, *Clin. Toxicol.* 37 (1999) 173–194.
- [4] J.M. Meichtry, M. Brusa, G. Mailhot, M.A. Grela, M.I. Litter, *Appl. Catal. B* 71 (2007) 101–107.
- [5] V.N.H. Nguyen, R. Amal, D. Beydoun, *Chem. Engg. Sci.* 58 (2003) 4429–4439.
- [6] M.I. Litter, *Appl. Catal. B* 23 (1999) 89–114.
- [7] M. Qamar, C.R. Yoon, H.J. Oh, N.H. Lee, K. Park, D.H. Kim, K.S. Lee, W.J. Lee, S.J. Kim, *Catal. Today* 131 (2008) 3–14.
- [8] M.R. Hoffmann, S.T. Martin, W. Choi, D.W. Bahnemann, *Chem. Rev.* 95 (1995) 69–94.
- [9] M. Muneer, D.W. Bahnemann, M.A. Tariq, M. Faisal, *Appl. Catal. A* 289 (2005) 224–230.
- [10] P.V. Kamat, *J. Phys. Chem. C* 111 (2007) 2834–2860.
- [11] M. Qamar, S.J. Kim, A.K. Ganguli, *Nanotechnology* 20 (2009) 455703–455710.
- [12] A.V. Vorontsov, V.P. Dubovitskaya, *J. Catal.* 221 (2004) 102–107.

- [13] A. Nakajima, H. Obata, Y. Kameshima, K. Okada, *Catal. Commun.* 6 (2005) 716–718.
- [14] V. Latour, T. Pigot, P. Mocho, S. Blanc, S. Lacomb, *Catal. Today* 101 (2005) 359–367.
- [15] C.S. Turchi, D.F. Ollis, *J. Catal.* 122 (1990) 178–181.
- [16] R.W. Matthews, S.R. McEvoy, *J. Photochem. Photobiol. A: Chem.* 64 (1992) 231.
- [17] H. Li, Z. Bian, J. Zhu, Y. Huo, H. Li, Y. Lu, *J. Am. Chem. Soc.* 129 (2007) 4538–4539.
- [18] K.M. Parida, N. Sahu, *J. Mol. Catal. A* 287 (2008) 151–158.
- [19] A. Idris, N. Hassan, N.S.M. Ismail, E. Misran, N.M. Yusof, A. Ngomsik, A. Bee, *Water Res.* 44 (2010) 1683–1688.
- [20] D.P. Das, K. Parida, B.R. De, *J. Mol. Catal. A* 245 (2006) 217–224.
- [21] J. Giménez, M.A. Aguado, S. Cervera-March, *J. Mol. Catal. A* 105 (1996) 67–78.
- [22] H. Fu, G. Lu, S. Li, *J. Photochem. Photobiol. A* 114 (1998) 81–88.
- [23] G. Coloin, M.C. Hidalgo, J.A. Naviño, *J. Photochem. Photobiol. A* 138 (2001) 79–85.
- [24] S.G. Schrank, H.J. Josefi, R.F.P.M. Moreira, *J. Photochem. Photobiol. A* 147 (2002) 71–76.
- [25] J.J. Testa, M.A. Grela, M.I. Litter, *Environ. Sci. Technol.* 38 (2004) 1589–1594.
- [26] T. Mishra, J. Hait, N. Aman, R.K. Jana, S. Chakravarty, *J. Colloid Interface Sci.* 316 (2007) 80–84.
- [27] M. Qamar, M.A. Gondal, K. Hayat, Z.H. Yamani, K. Al-Hooshani, *J. Hazard. Mater.* 170 (2009) 584–589.
- [28] A. Hameed, M.A. Gondal, *J. Mol. Catal. A* 233 (2005) 35–41.
- [29] JCPDS. No. 25-582.
- [30] X. Wang, J. Song, L. Gao, J. Jin, H. Zheng, Z. Zhang, *Nanotechnology* 16 (2005) 37.
- [31] C.C. Wang, Z. Zhang, J.Y. Ying, *Nanostruct. Mater.* 9 (1997) 583.
- [32] S. Chakrabarti, B.K. Dutta, *J. Hazard. Mater.* 112 (2004) 269–275.
- [33] C.R. Chenthamarakshan, Y. Hui, Y. Ming, K. Rajeshwar, *J. Electroanal. Chem.* 494 (2000) 79–86.